

## Pressure-induced negative charge state of the $EL2$ defect in its metastable configuration

Michał Baj

*Institute of Experimental Physics, University of Warsaw, Hoża 69, PL-00-681 Warsaw, Poland*

Piotr Dreszer

*High Pressure Research Center "Unipress," Polish Academy of Sciences, Sokołowska 29/37, PL-01-142 Warsaw, Poland*

Adam Babiński

*Institute of Experimental Physics, University of Warsaw, Hoża 69, PL-00-681 Warsaw, Poland*

(Received 6 August 1990)

We present the results of electrical-conductivity and low-temperature deep-level transient spectroscopy (DLTS) measurements performed with use of monochromatic light at hydrostatic pressures up to 0.7 GPa on  $n$ -type GaAs samples containing the  $EL2$  defect. Based on our results we give clear experimental evidence that there exists an acceptorlike level of the metastable  $EL2$  configuration. Without pressure this level is resonant with the conduction band and therefore unoccupied, but under pressure it enters the energy gap capturing free electrons and leading to the negative charge state of the metastable  $EL2$ . The electrical activity of the level manifests itself in optically induced persistent changes of the electrical conductivity and DLTS signal, driven by  $EL2$  photoquenching and extremely efficient  $EL2$  photorecovery processes. These effects vanish at the temperature at which  $EL2$  thermally recovers its normal configuration. We exclude the "negative- $U$ " case for the level and determine its energetic position and the pressure shift. We claim that the negative charge state of the metastable  $EL2$  is responsible for the optical accessibility of the metastable configuration. Finally, we refer the experimentally confirmed existence of this level to the predictions of the  $EL2$  theoretical models.

### I. INTRODUCTION

The main native defect present in GaAs,  $EL2$ , belongs to one of the most intensely studied defects in III-V semiconducting compounds. It is well known that the  $EL2$  defect possesses a midgap donor level  $(EL2)^{0/+}$  (Refs. 1–4) which in  $n$ -type GaAs is fully occupied and therefore the  $EL2$  is in its neutral charge state,  $(EL2)^0$ . This charge state manifests itself in a very characteristic absorption spectrum consisting of the photoionization background and the intra- $(EL2)^0$  absorption band.<sup>5–7</sup> At low temperatures this absorption can be completely quenched by means of irradiation with photons in the energy range 1–1.35 eV.<sup>8,9</sup> The ability to undergo this photoinduced transformation (without the change of the  $EL2$  charge state<sup>3,10,11</sup>) from the normal configuration to the metastable  $(EL2)^*$  one is one of the most intriguing properties of the  $EL2$  defect. It is commonly believed that the photon-created metastable configuration,  $(EL2)^*$ , apparently exhibits no experimentally observed properties of its own—no electrical<sup>11</sup> and electron paramagnetic resonance (EPR) (Refs. 4 and 12–14) activity as well as no clear optical accessibility.<sup>15</sup>

The  $EL2$  defect recovery from the metastable configuration  $(EL2)^*$  to the normal one can be induced by means of thermal annealing of a crystal up to temperatures highly dependent on the free-electron concentration: 140 K for a semi-insulating material and 50 K for an  $n$ -type one.<sup>16–20</sup> The photoinduced recovery processes have also been reported, but their efficiencies were

much lower than those of the photoquenching processes and most of these effects were only partial.<sup>19,21–28</sup>

In a recent paper,<sup>29</sup> we gave experimental evidence that in semi-insulating as well as in  $n$ -type GaAs under hydrostatic pressure the metastable configuration  $(EL2)^*$  became optically accessible with an extremely efficient purely optical recovery process that was not observed without pressure. This process appeared gradually at pressures 0.25–0.3 GPa, and then at  $p > 0.3$  GPa the experimental results were qualitatively the same irrespective of pressure. The  $(EL2)^0$ -related spectrum could be reversibly photoquenched and fully recovered many consecutive times, even at low temperature  $T = 5$  K. The efficiency of this recovery process for photons from the energy range slightly below band-to-band transitions was comparable to, and for  $n$ -type GaAs even exceeded, the efficiency of the  $EL2$  photoquenching process. Moreover, in  $n$ -type samples, contrary to the semi-insulating material, after the  $EL2$  photoquenching there appeared a weakly dispersive additional absorption clearly anticorrelated to the  $(EL2)^0$ -related absorption band. We proposed that this absorption was the photoionization of the  $EL2$  defect being in its metastable configuration with an additional electron trapped on it. The capture of an extra electron by  $EL2$  resulting in the negatively charged state  $[(EL2)^*]^-$  had to be easily detectable by electrical measurements.

The aim of the present high-pressure investigations was to check the above suggestion. Based on the results of our electrical conductivity and deep-level transient spec-

troscopy (DLTS) measurements performed with an access of monochromatic light, we provided clear experimental evidence that the metastable  $EL2$  defect possessed an acceptorlike level that was resonant with the conduction band without pressure and entered the energy gap at high pressure. This level creates the electrical activity and optical accessibility of the  $EL2$  metastable configuration at high pressure, which seems to be of crucial importance in solving the problem of the microscopic model of the  $EL2$  defect and the mechanism of its metastability.

## II. EXPERIMENT

We investigated two kinds of horizontal Bridgman-grown  $n$ -type GaAs samples. Their electronic-transport parameters are given in Table I. The samples were chosen in such a way that the  $EL2$ -defect concentration  $N_{EL2}$  was either approximately two times higher (sample no. 1) or lower (sample no. 2) than the free-electron concentration  $n_{300\text{ K}}$  (see Table I). In both samples we observed that the Hall concentration  $n = 1/eR_H$  decreased during cooling the samples in the dark down to approximately 40 K and then increased sharply to the values close to  $n_{300\text{ K}}$  (see Fig. 1). At the same time the Hall mobility  $R_H\sigma$  decreased several times in the range 20–50 K and then it became temperature independent. This means that in our samples at high temperatures the electronic transport took place mainly in the conduction band and the observed temperature dependence of the Hall concentration was due to the freezing of free carriers onto the impurity band of shallow donors, while at low temperatures the transport took place in the impurity band itself. However, without illumination in the whole temperature range the total concentration of the conducting electrons (hereafter denoted also as free electrons) remained constant.

We performed electrical conductivity and DLTS measurements at temperatures ranging from 5 to 70 K and hydrostatic pressures up to 0.7 GPa with an access of monochromatic light. Samples were placed in a high-pressure optical cell with helium as a pressure transmitting medium. At high pressure, helium solidified (or melted) in the temperature range of interest, which resulted in the abrupt change of pressure in our pressure cell. Therefore we tried to avoid the disadvantage of crossing the phase-transition temperature during our experimental temperature transients (the only exception was the experiment presented in Fig. 6) so as to deal with

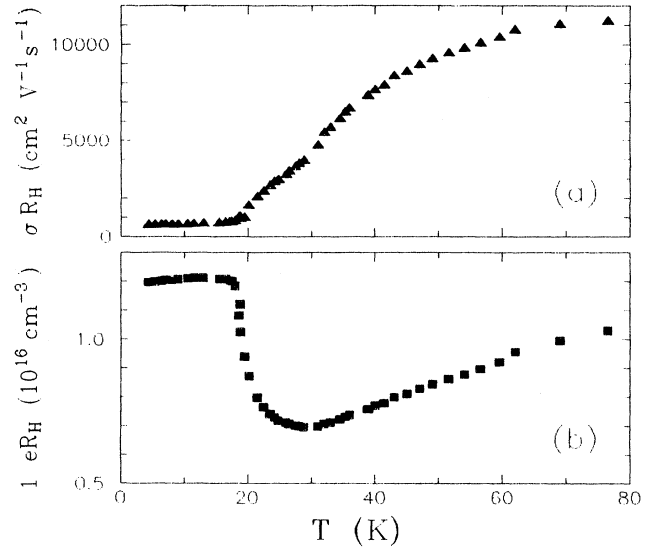


FIG. 1. The Hall mobility (a) and the Hall concentration (b) of sample no. 1 measured in the dark at  $p = 0.3$  GPa without any previous illumination.

either gaseous or solid helium. A tungsten halogen lamp and a prism or grating monochromator were employed to illuminate the samples. The sample temperature could be kept constant within 0.1 K. The electrical conductivity measurements were done with a four-probe method with indium contacts in the van der Pauw configuration. For DLTS measurements a lock-in amplifier-based system was used. Schottky diodes were fabricated by Au evaporation on a GaAs surface, degreased and etched in diluted HCl. The thickness of all the samples for conductivity as well as DLTS measurements did not exceed 1.5 mm.

## III. RESULTS AND DISCUSSION

### A. Pressure-induced persistent photoconductivity

It is commonly believed that the  $EL2$  defect, while being in its metastable configuration ( $EL2$ )\*, is in the neutral [ $(EL2)^*$ ]<sup>0</sup> charge state and the photoquenching of ( $EL2$ )<sup>0</sup> as well as thermal recovery [ $(EL2)^* \rightarrow EL2$ ] processes take place without the change of the  $EL2$  charge state.<sup>3,10,11</sup> The existence of charge states of ( $EL2$ )<sup>\*</sup> oth-

TABLE I. Characteristics of the investigated samples.

Sample	Dopant	$n_{300\text{ K}}$ ( $10^{16}\text{ cm}^{-3}$ )	$\mu_{300\text{ K}}$ ( $\text{cm}^2\text{ V}^{-1}\text{ s}^{-1}$ )	$\sigma_{300\text{ K}}$ ( $\Omega^{-1}\text{ cm}^{-1}$ )	$\sigma_{4.2\text{ K}}$ ( $\Omega^{-1}\text{ cm}^{-1}$ )	$N_{EL2}$ ( $10^{16}\text{ cm}^{-3}$ )	$k = N_{EL2}/n_{300\text{ K}}$
no. 1 GaAs	Si	1.2 <sup>a</sup>	5550	10.8	2.2	2.7 <sup>b</sup>	2.3
no. 2 GaAs	none	3.2 <sup>a</sup>	4480	22.8	5.9	1.3 <sup>c</sup>	0.41

<sup>a</sup>Determined from Hall effect measurements.

<sup>b</sup>Determined from the intensity of the ( $EL2$ )<sup>0</sup> zero-phonon-line absorption (Ref. 30).

<sup>c</sup>Evaluated from the standard DLTS measurements.

er than the neutral one  $[(EL2)^*]^0$  has not yet been reported. However, in a recent paper<sup>29</sup> we suggested that under hydrostatic pressure exceeding 0.25–0.3 GPa the metastable  $(EL2)^*$  might capture an additional electron leading to an  $[(EL2)^*]^-$  negative charge state. This should introduce persistent changes of the free-electron concentration and, as a consequence, the electrical conductivity of a sample must be strongly dependent on the distribution of the  $EL2$  defects between its normal and metastable configurations. In an attempt to verify this hypothesis, we investigated at low ( $T \approx 5$  K) and constant temperature the conductivity transients of the samples during successive photoquenching and photorecovery processes. The exemplary results obtained at high pressure for both samples no. 2 and 1 are presented in Figs. 2 and 3, respectively. These results can be described as follows.

(i) At sufficiently high hydrostatic pressure ( $p \geq 0.25$  GPa) the optically induced ( $h\nu = 1.17$  eV) transfer of the  $EL2$  to its metastable configuration caused the drop of the conductivity of both samples. For sample no. 2, for which  $N_{(EL2)^0}/n_{300\text{ K}} \approx 0.4$ , and only a part of the free electrons could be trapped on  $(EL2)^*$  leading to its negatively charged state  $[(EL2)^*]^-$ , the value of the conductivity obtained after the full  $EL2$  photoquenching was about two times lower than the initial one (see Fig. 2). In the case of sample no. 1, for which  $N_{(EL2)^0}/n_{300\text{ K}} \approx 2.3$  and all the free electrons could be bound by  $(EL2)^*$ , we observed a drastic fall of the conductivity (see Fig. 3), exceeding seven orders of magnitude and leading to immeasurably high resistance of the sample (light-induced metal-insulator transition).

(ii) The highly conductive state of the samples could be fully restored by illumination with light from the spectral range from approximately 1.4 eV to the energy of band-to-band transitions (see Figs. 2 and 3). This effect is fully analogous to the optically induced recovery of the  $(EL2)^0$  intracenter absorption, observed previously.<sup>29</sup> Thus, it should be interpreted as a photorecovery of the  $EL2$  defect from its metastable, negatively charged state  $[(EL2)^*]^-$  to the neutral normal one  $(EL2)^0$  with an accompanying process of releasing an extra electron trapped by  $EL2$ :  $[(EL2)^*]^- + h\nu \rightarrow (EL2)^0 + e^-$ . The efficiency of this photorecovery process was very high—for photons with energies near the band-to-band transitions, the efficiency even exceeded that of the photoquenching process (see Figs. 2 and 3).

(iii) The main contribution to the light-induced electrical conductivity changes was persistent (i.e., the conductivity of the samples retained its value after the irradiation was interrupted), however a nonpersistent photoconductivity, originating from band-to-band transitions, was also noticeable (see Figs. 2 and 3).

(iv) The conductivity changes were fully reversible, i.e., the experimental procedure of the successive photoquenching and photorecovery processes could be reproducibly repeated many times one after the other.

(v) None of the phenomena described above were observed at ambient pressure; they then gradually appeared with increasing pressure, but at  $p > 0.3$  GPa the experimental results were qualitatively the same irrespective of

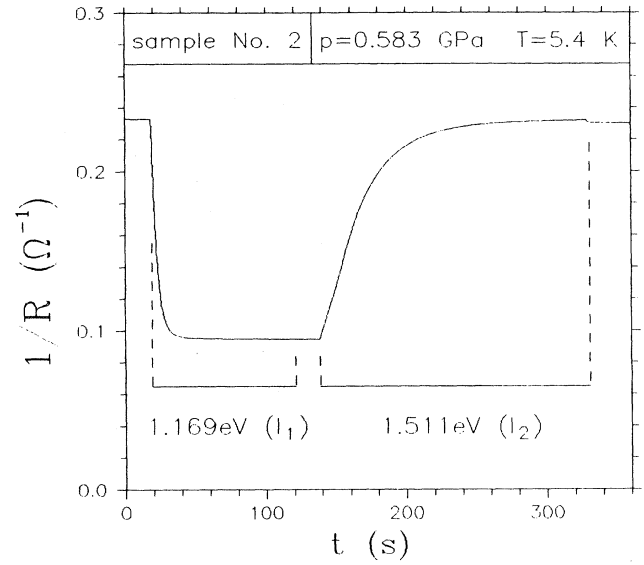


FIG. 2. The transient of the electrical conductance of sample no. 2 recorded at  $p = 0.583$  GPa and  $T = 5.4$  K during successive optical  $EL2$  quenching ( $h\nu = 1.169$  eV) and optical  $EL2$  recovery ( $h\nu = 1.511$  eV) processes. The ratio of the monochromatic light intensities was  $I_1:I_2 = 5:1$ .

pressure.

The full analogy between the above experimental findings and the results of our previous paper<sup>29</sup> [where the  $(EL2)^0$  intracenter absorption was measured instead of the electrical conductivity] means that at  $p > 0.3$  GPa,  $EL2$  photorecovery and photoquenching processes as well as the distribution of the  $EL2$  defects between their normal and metastable configurations can be monitored

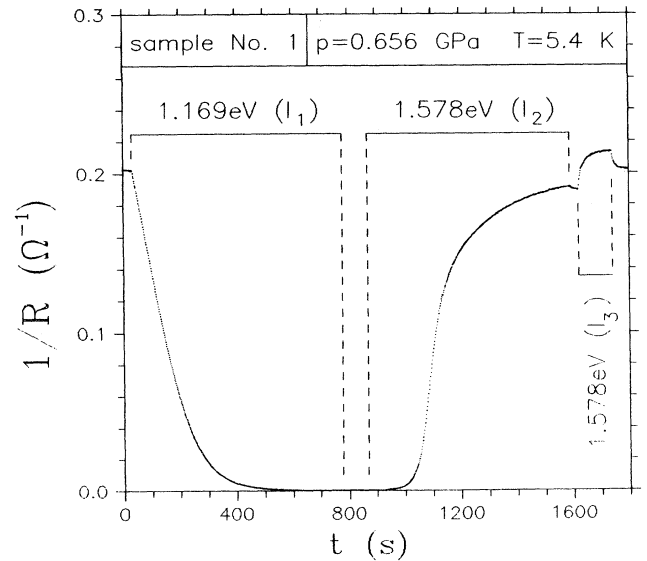


FIG. 3. The transient of the electrical conductance of sample no. 1 recorded at  $p = 0.656$  GPa and  $T = 5.4$  K during successive optical  $EL2$  quenching ( $h\nu = 1.169$  eV) and optical  $EL2$  recovery ( $h\nu = 1.578$  eV) processes. The ratio of the monochromatic light intensities was  $I_1:I_2:I_3 = 5:1:11$ .

both by electrical conductivity and optical-absorption measurements. Thus it was possible to observe the  $EL2$  thermal recovery process [usually monitored by the  $(EL2)^0$  intracenter absorption<sup>18,19</sup>] in our electrical conductivity,  $\sigma$ , measurements; see Fig. 4, in which we present the temperature transients of  $\sigma$  of the sample no. 1 after the initial  $EL2$  photoquenching, performed at  $T=10$  K. The highly resistive state of the sample persisted up to about 40 K and then the thermally induced  $[(EL2)^*]^- \rightarrow (EL2)^0$  transformation released the electrons to the conduction band, so that  $\sigma$  increased sharply. The further small increase ( $T > 48$  K) of  $\sigma$  is due to the change of the electron mobility only; see Fig. 1.

Our experimental results presented in this section provide convincing arguments that the  $[(EL2)^*]^{-/0}$  acceptorlike level [i.e., the level of the photon-created metastable  $(EL2)^*$  configuration] is resonant with the conduction band at ambient pressure and at  $p \geq 0.25$  GPa enters the energy gap capturing free electrons. The following sections give further confirmations of this statement.

### B. Low-temperature DLTS experiments at high pressure

Since the optical transformation of the  $EL2$  defect to its metastable configuration creates the acceptorlike  $[(EL2)^*]^{-/0}$  level, which at  $p \geq 0.25$  GPa traps free electrons, this level should be detectable by means of the DLTS technique. Since even at the highest applied pressure the level cannot lie deep in the energy gap and it only exists as long as the  $EL2$  defect is in its metastable configuration (that is, at  $T < 40$  K), the DLTS measurements had to be performed at low temperatures.

The experiment was done on sample no. 2 because its electrical conductivity always remained high enough, ir-

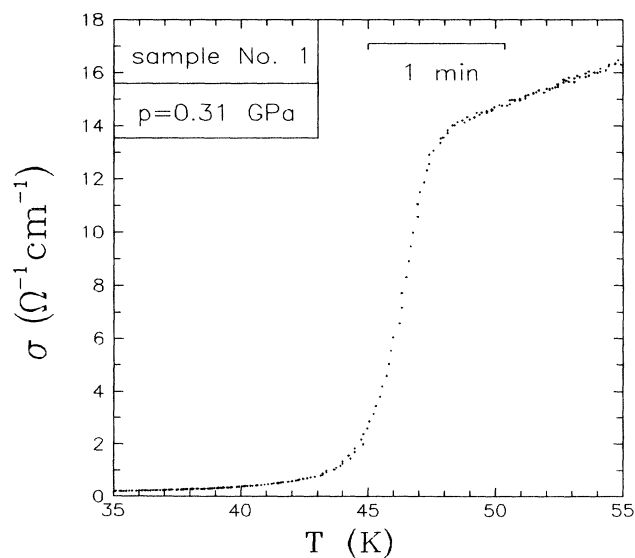


FIG. 4. The temperature transients of the electrical conductivity of sample no. 1 measured at  $p=0.31$  GPa during heating of the crystal.  $EL2$  was initially fully photoquenched at  $T=5$  K by means of long-time (10 min) illumination ( $h\nu=1.17$  eV); see text.

respective of the distribution of the  $EL2$  defects between their normal and metastable configurations (see Fig. 2). The experimental procedure consisted of the following irradiation cycles: (i) the DLTS spectrum measurement up to 40 K and the subsequent cooling of the sample down to 10 K; (ii) monochromatic light irradiation of the sample (photoquenching or photorecovery of the  $EL2$ ); (iii) the same as (i) to verify the influence of the irradiation. The results obtained by means of such a procedure are presented in Fig. 5. The initial DLTS run (curve *a* of Fig. 5) was made after cooling the Schottky diode down from room temperature to 10 K in the dark with the zero bias (however, the result was not affected by the applied bias voltage). Since in this situation there was no  $EL2$  in its metastable configuration, the  $[(EL2)^*]^{-/0}$  level did not exist and hence there was no DLTS signal either. However, after the  $EL2$  photoquenching ( $h\nu=1.13$  eV) there appeared a signal with the DLTS peak close to  $T=32$  K (see curve *b* of Fig. 5). Then subsequent  $EL2$  photorecovery ( $h\nu=1.57$  eV) reduced the DLTS signal intensity partially or almost fully, depending on the irradiation time; see spectra *c* and *d* in Fig. 5. The high DLTS signal was then restored after the repeated  $EL2$  photoquenching (spectrum *e* in Fig. 5). The observed correlation between the DLTS signal intensity and the concentration of the  $EL2$  being in its metastable configuration strongly supports the identification of the level as the  $[(EL2)^*]^{-/0}$  one. The  $EL2$  photoquenching increases the concentration of  $(EL2)^*$ , so the DLTS signal, which is due to the  $[(EL2)^*]^{-/0}$  level, also increases, while at

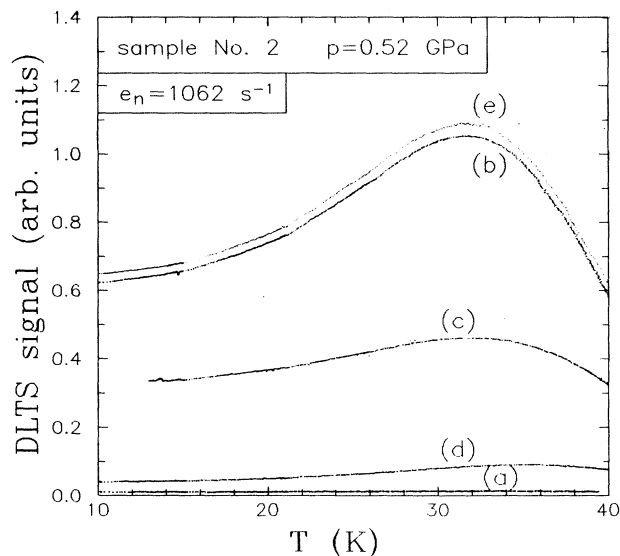


FIG. 5. The influence of the successive processes of the monochromatic light irradiation performed at  $T=5$  K and  $p=0.52$  GPa on the DLTS spectra for sample no. 2: *a*, initial DLTS spectrum after cooling the sample down to 5 K in the dark; *b*, after  $h\nu=1.13$  eV  $EL2$  photoquenching for 10 min; *c*, after  $h\nu=1.57$  eV partial  $EL2$  photorecovery for 5 min; *d*, the same as *c* after the next 5 min; *e*, after repeated  $h\nu=1.13$  eV  $EL2$  photoquenching for 10 min. The reverse bias was  $-0.5$  V, the pulse amplitude was  $0.5$  V, and the emission rate window  $e_n=1062$  s<sup>-1</sup>.

the same time the free-electron concentration and the electrical conductivity decrease, because of the trapping of free electrons by the level (see Sec. III A). The photo-recovery involves reverse changes of the DLTS signal and the electrical conductivity.

The pressure evolution of the DLTS spectra collected after the full *EL2* photoquenching at three different pressures is presented in Fig. 6. It is clearly seen that the position of the DLTS peak shifted to higher temperatures with increasing hydrostatic pressure, reflecting the pressure-induced movement of this level down with respect to the bottom of the conduction band. Unfortunately, because of the unusual asymmetric shape of the DLTS peak, we could not determine reliably the activation energy of the  $[(EL2)^*]^{-/0}$  level and its pressure shift from our DLTS data. It should be noted that even at the lowest temperatures we observed a pronounced DLTS signal that decreased at higher pressures, while the intensity of the DLTS peak increased at the same time. Moreover, we found that the higher the Schottky diode reverse voltage or the lower the filling pulse frequency was, the more asymmetric the DLTS spectrum shape was. It seems that the observed unusual shape of the spectra originated from the temperature-independent electric field emission<sup>31–33</sup> of the electrons from the relatively shallow  $[(EL2)^*]^{-/0}$  level. This effect should decrease for lower bias voltages as well as for higher pressures at which the level becomes deeper. Therefore, this could explain the experimental findings concerning the shape of the DLTS spectra. In addition, there is another intriguing fact that needs further study, namely that the observed DLTS signal was by far too low in comparison with the total *EL2* concentration.

In our DLTS measurements, periodically repeated

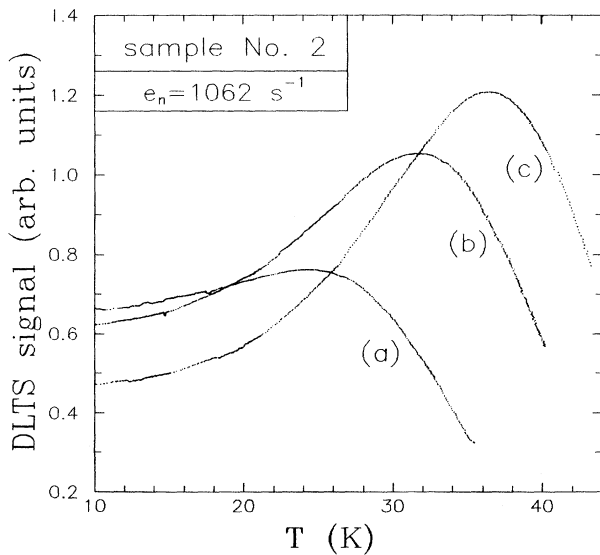


FIG. 6. The pressure evolution of the DLTS spectra collected after the full *EL2* photoquenching ( $h\nu=1.17$  eV, 10 min) at three different pressures: spectrum *a* at  $p=0.4$  GPa, spectrum *b* at  $p=0.5$  GPa, and spectrum *c* at  $p=0.6$  GPa. The reverse bias was  $-0.5$  V, the pulse amplitude was  $0.5$  V, and the emission rate window  $e_n=1062$  s<sup>-1</sup>.

filling pulses induced free carriers to the space-charge region of the Schottky diode, therefore the *EL2* defect in the junction should thermally recover to its normal configuration in the same temperature range as in the bulk *n*-type material (i.e., at 40–50 K).<sup>18–20</sup> Such a thermal recovery, monitored with the DLTS signal, is presented in Fig. 7. After the optical quenching of the *EL2* at  $T=10$  K, we performed the DLTS run up to about 60 K. The results up to 40 K were quite similar to those shown in Figs. 5 and 6. Then, because of the melting of helium in the pressure cell, we observed an abrupt increase of pressure that induced the shift of the peak position originating from the pressure-induced movement of the  $[(EL2)^*]^{-/0}$  level. Starting from  $T=44$  K, the pressure transmitting medium was already gaseous and the DLTS spectrum was again smooth. At  $T=46$  K the signal began to fall drastically and at  $T=56$  K its value almost reached zero. This drop was irreversible (unlike the case of the change of the DLTS signal observed below 40 K), which is illustrated by the lack of the DLTS signal during the subsequent cooling down of the sample. It originates from the absence of the electrically active  $[(EL2)^*]^{-/0}$  level after the thermal recovery of the *EL2*. This is consistent with our electrical conductivity measurements; see Sec. III A and Fig. 4.

The results of the present section confirm the existence of the  $[(EL2)^*]^{-/0}$  level, which is responsible for the observed DLTS spectra. The pressure evolution of the DLTS peak seen in Fig. 5 indicates that the level moves down with respect to the conduction-band edge.

### C. Thermal population of the $[(EL2)^*]^{-/0}$ level

In the preceding sections we proved that at high pressure and low temperature the relatively shallow  $[(EL2)^*]^{-/0}$  level traps free electrons, which results in

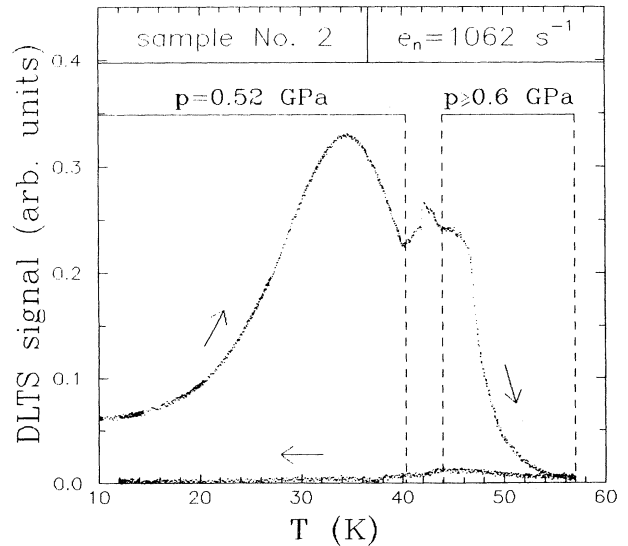


FIG. 7. The thermal recovery of the *EL2* defect monitored with the DLTS signal; see text. The reverse bias was  $-0.1$  V, the pulse amplitude was  $0.1$  V, and the emission rate window  $e_n=1062$  s<sup>-1</sup>.

the electrical conductivity changes. Therefore at constant pressure the population of the level and thus the concentration of conducting electrons should be very sensitive to the sample temperature.

We investigated the temperature dependences of the electrical conductivity,  $\sigma$ , of sample no. 1 up to 30 K at three different constant pressures. We tried to avoid both the *EL2* thermal recovery process and the crossing of the He melting point, which defined the upper temperature limit for each measurement. The Arrhenius plots of the experimental data obtained after the full *EL2* photoquenching are given in Fig. 8. In the whole temperature range,  $\sigma$  was thermally activated with the activation energy increasing from approximately 0.8 meV for  $p=0.25$  GPa to about 10 meV for  $p=0.45$  GPa, which reflects the pressure shift of the thermal ionization energy of the  $[(EL2)^*]^{-/0}$  level. Moreover, it should be pointed out that the conductivity at a given pressure was a unique function of temperature, i.e., the results obtained during the heating or cooling of the sample were the same even at the lowest temperatures. This means that the  $[(EL2)^*]^{-/0}$  level was always in the thermal equilibrium with the conduction band and hence the change of the charge state within the *EL2* metastable configuration  $[(EL2)^*]^{-} \leftrightarrow [(EL2)^*]^0$  takes place without an additional strong lattice relaxation, i.e., these charge states are separated by a configuration barrier.

#### D. Pressure-induced changes of the thermal population of the $[(EL2)^*]^{-/0}$ level

The applied hydrostatic pressure strongly influences the energetic position of the  $[(EL2)^*]^{-/0}$  level with respect to the bottom of the conduction band and, as a consequence, it modifies the thermal equilibrium between the level and the conduction band. The equilibrium pop-

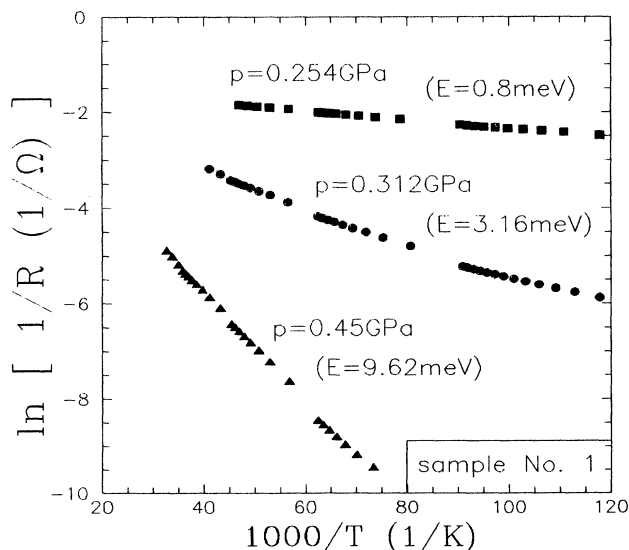


FIG. 8. The Arrhenius plots of the electrical conductance of sample no. 1 measured at three different constant pressures after the full *EL2* photoquenching ( $h\nu=1.17$  eV, 10 min) with the estimated activation energies.

ulation of the level can be monitored by electric conductivity,  $\sigma$ , measurements.

We studied the isothermal pressure dependences of  $\sigma$  for various concentration of the metastable  $(EL2)^*$ . In these experiments we chose the relatively high temperature  $T=35.1$  K at which we could easily change and control the pressure up to 0.4 GPa in the gaseous helium as a pressure transmitting medium. On the other hand, this temperature was sufficiently low to avoid the thermal *EL2* recovery process. The results are presented in Fig. 9 for sample no. 2 and in Figs. 10 and 11 for sample no. 1. We would like to point out the following.

(i) As long as the *EL2* was in its normal configuration,  $\sigma$  depended on pressure very weakly and linearly, which was due to a small pressure-induced decrease of electron mobility only (see Figs. 9–11).

(ii) When the *EL2* was partially or fully transformed to its metastable configuration,  $\sigma$  was strongly pressure-dependent, however for a given sample,  $\sigma$  at low pressure was practically the same, irrespective of the actual distribution of the *EL2* between its normal and metastable configurations. This reflects the fact that without pressure both *EL2* and  $(EL2)^*$  are in *n*-type GaAs in their neutral charge states. The higher the pressure was, the lower the energy of the level was in respect to the bottom of the conduction band and the lower the free-electron concentration (or  $\sigma$ ) was because the population of the  $[(EL2)^*]^{-/0}$  level increased; see Figs. 9–11.

(iii) We distinguished two kinds of  $\sigma(p)$  dependences: (a) the steplike shape [see Fig. 9 and curve 2 in Fig. 10(a)] when at the highest pressure  $\sigma$  was practically saturated with relatively high value; (b) the shape without a high-pressure saturation [see curve 3 in Fig. 10(b)]. The first shape was always observed for sample no. 2, for which  $n_{300\text{ K}} > N_{EL2}$ , and for sample no. 1 after partial photo-

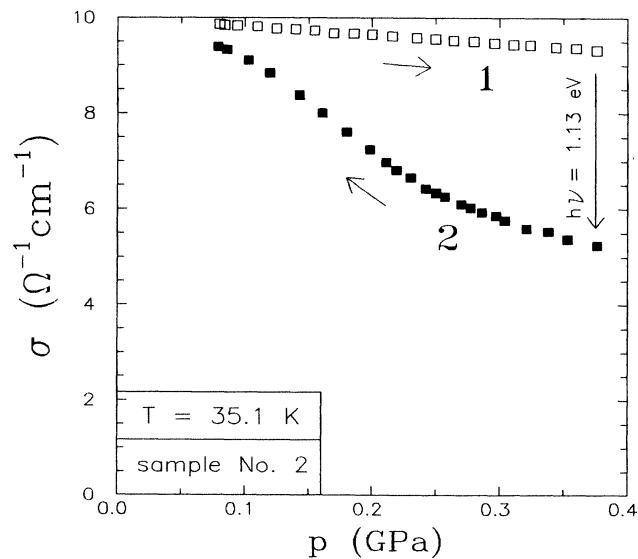


FIG. 9. Pressure dependence of the electrical conductivity of sample no. 2 measured at  $T=35.1$  K before (open squares, curve 1) and after (solid squares, curve 2) the full *EL2* photoquenching with  $h\nu=1.13$  eV for 10 min. The arrows depict the direction of the pressure changes.

quenching only. In this case at the highest pressure the population of the  $[(EL2)^*]^{-/0}$  level was practically saturated and thus the height of the step was proportional to  $N_{[(EL2)^*]^{-}} \approx N_{(EL2)^*}$ . The second shape was observed only for sample no. 1 with a sufficiently high concentration of photon-created  $(EL2)^*$ . Since for this sample  $n_{300\text{ K}} < N_{EL2}$ , the population of the  $[(EL2)^*]^{-/0}$  level was not full in this case and a part of the  $(EL2)^*$  always remained in its neutral charge state.

(iv) The  $\sigma(p)$  dependences were quantitatively the same, irrespective of the pressure (low or high) at which

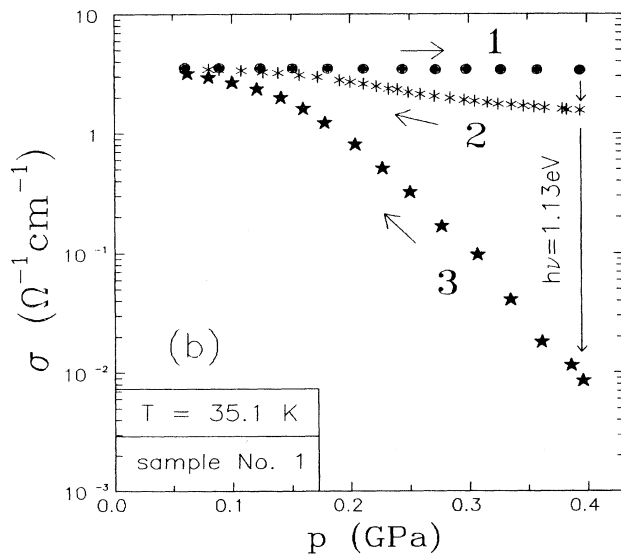
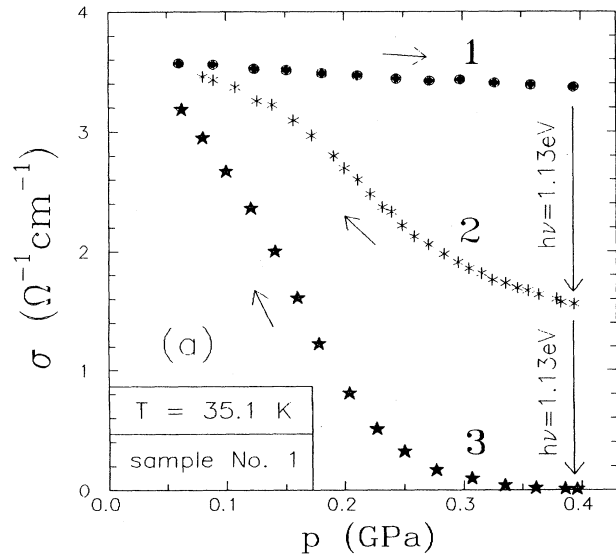


FIG. 10. Pressure dependence of the electrical conductivity of sample no. 1 measured at  $T=35.1\text{ K}$  before (solid circles, curve 1), after partial (asterisks, curve 2), and full (stars, curve 3)  $h\nu=1.13\text{ eV}$   $EL2$  photoquenching presented in (a) a linear scale and (b) a semilogarithmic one. The arrows depict the direction of the pressures changes.

the  $EL2$  defect was photoquenched; compare curve 3 in Fig. 10(b) with curve 2 in Fig. 11.

(v) Even at the lowest applied pressure  $p < 0.1\text{ GPa}$ , the temperature ( $35.1\text{ K}$ ) was high enough to partially populate the  $[(EL2)^*]^{-/0}$  level, which at low pressure was resonant but very close to the bottom of the conduction band; the values of  $\sigma$  were noticeably different before and after  $EL2$  photoquenching.

All the above results point out that under hydrostatic pressure there exists a very curious and unique possibility of controlling (via  $EL2$  photoquenching and photorecovery processes) the concentration of the defect centers (i.e., the  $EL2$  defects in their metastable configurations) which can bind free electrons on the localized electronic state (the  $[(EL2)^*]^{-/0}$  level).

### E. The $[(EL2)^*]^{-/0}$ level energy and its pressure dependence

In this section we will estimate the energy of the  $[(EL2)^*]^{-/0}$  level, hereafter denoted as  $\varepsilon^{-/0}$ , and its pressure shift. First it should be pointed out that  $[(EL2)^*]^{-/0}$  level is the proper level of the metastable configuration of the  $EL2$  defect. This means that  $\varepsilon^{-/0}$ , given in respect to the bottom of the conduction band, is the energy yield obtained from the change of the total energy (electronic + elastic) of the metastable  $EL2$  upon the transfer of the electron from the negatively charged state  $[(EL2)^*]^{-}$  to the bottom of the conduction band leading to the neutral charge state, but still within the metastable configuration  $[(EL2)^*]^0$ :

$$\varepsilon^{-/0} = E_{-}^{*} - E_{0}^{*}, \quad (1)$$

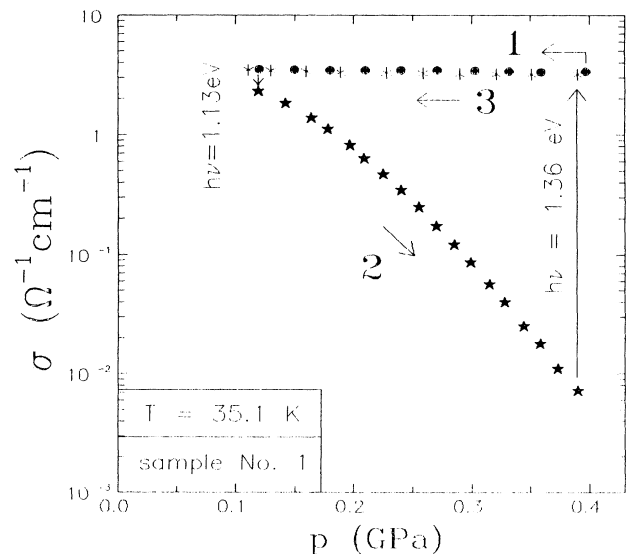


FIG. 11. Pressure dependence of the electrical conductivity of sample no. 1 measured at  $T=35.1\text{ K}$  before (solid circles, curve 1) and after (stars, curve 2) full  $h\nu=1.13\text{ eV}$   $EL2$  photoquenching and then after successive (asterisks, curve 3) full  $h\nu=1.36\text{ eV}$   $EL2$  photorecovery. The arrows depict the direction of the pressures changes.

where  $E^*$  is the total energy of the negatively charged defect and  $E_0^*$  that of the neutral defect with an electron at the bottom of the conduction band. Both energies refer to the defect being in its metastable configuration,  $(EL2)^*$ , which can exist at  $T < 50$  K only.

The thermal ionization energy of the  $[(EL2)^*]^{-/0}$  level could not be determined from our DLTS data because of the asymmetric shape of the DLTS spectra; see Sec. III B. On the other hand, the temperature variation of the electron mobility (see Fig. 1) strongly affected our  $\sigma(T)$  data presented in Sec. III C. Thus it was also not reasonable to use them for the accurate determination of the level energy  $\epsilon^{-/0}$ . The best solution seemed to be the application of our results obtained at a constant temperature  $T=35.1$  K, i.e., the pressure dependences of  $\sigma$  (see Sec. III D), because the pressure dependence of the electron mobility at  $T=35.1$  K was very weak and practically linear [see curves “1” in Figs. 9 and 10(a)].

For the quantitative analysis we chose the experimental results presented as curve “2” in Fig. 9 (for sample no. 2) and curve “2” in Fig. 10(a) (for sample no. 1). Since in our optical pressure cell we were able to measure the electrical conductivity  $\sigma$ , but not the free-electron concentration  $n$ , we tried to recalculate  $\sigma$  onto  $n$ . To evaluate the relative pressure changes of  $n$  [ $n_{35\text{ K}}(p)/n_{35\text{ K}}(p=0)$ ] we took into account the electron mobility changes for both samples by a simple division of each curve “2” by the corresponding curve “1.” Then, assuming that  $n_{35\text{ K}}(p=0) = n_{300\text{ K}}(p=0)$  (see Sec. II), we calculated the scaling factors for both samples, which enabled us to find the absolute values of  $n$  for every pressure. The results of the above procedure are presented in Fig. 12 as “experimental points.”

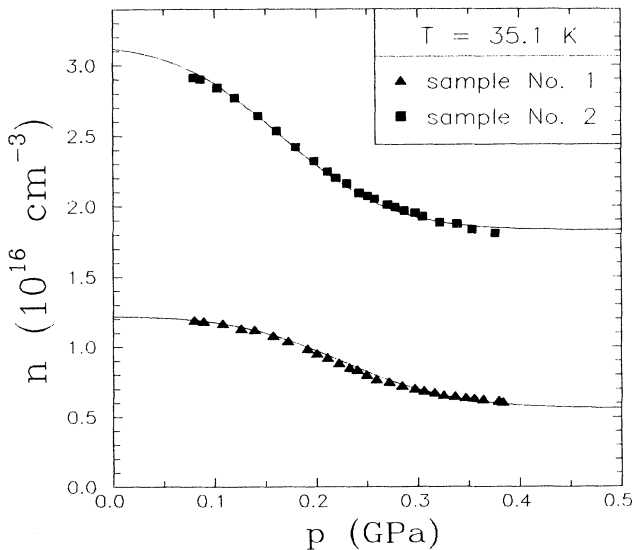


FIG. 12. The hydrostatic pressure dependence of the free-electron concentration after full  $EL2$  photoquenching for sample no. 2 (solid squares) and partial  $EL2$  photoquenching for sample no. 1 (solid triangles). The solid lines were fitted to experimental data in order to determine the  $[(EL2)^*]^{-/0}$  level energy and its pressure shift; see text.

The numerical analysis of these data was based on the following formulas.

(a) The equation describing the equilibrium population of the  $[(EL2)^*]^{-/0}$  level:

$$\frac{N_{[(EL2)^*]^-}}{N_{[(EL2)^*]^0}} = \exp \left[ \frac{E_F - \epsilon^{-/0} + T \Delta S}{k_B T} \right], \quad (2)$$

where  $N_{[(EL2)^*]^-}$  and  $N_{[(EL2)^*]^0}$  stand for the concentration of the metastable  $EL2$  in negative and neutral charge states, respectively;  $\Delta S$  is the local entropy change during the transition from  $[(EL2)^*]^0$  to  $[(EL2)^*]^-$ ;  $E_F$  is the Fermi level energy.

(b) The balance between various states of  $EL2$ :

$$N_{EL2} = N_{[(EL2)^*]^0} + N_{[(EL2)^*]^-} + N_{(EL2)^0}, \quad (3)$$

where  $N_{EL2}$  is the total  $EL2$  concentration and  $N_{(EL2)^0}$  represents the concentration of  $EL2$  being in its normal configuration (always neutral in our  $n$ -type samples).

(c) The charge balance of the sample

$$n + N_A + N_{[(EL2)^*]^-} = N_D, \quad (4)$$

where  $n$  is the free-electron concentration, and  $N_A$  and  $N_D$  are the concentrations of always ionized acceptors and shallow donors, respectively.

Equations (2)–(4) enabled us to calculate the free-electron concentration, which could then be compared with the experimental data from Fig. 12. To get the best agreement between the experiment and the results of calculation, we fitted two parameters,  $\epsilon^{-/0}(p=0)$  and  $\partial\epsilon^{-/0}/\partial p$ , common for both samples, and one additional parameter,  $N_{(EL2)^0}$ , for sample no. 1 only, for which the photoquenching process was not completed and  $N_{(EL2)^0} \neq 0$ . The total  $EL2$  concentration  $N_{EL2}$  was not fitted, but taken from standard DLTS measurements or absorption data (see Table I).

The following assumptions and/or simplifications were used in our calculations.

(i)  $N_D - N_A = n_{300\text{ K}}$ , which means that even at low temperature,  $T=35.1$  K, all the shallow donors and acceptors were ionized and the total concentration of conducting electrons, which could be captured by  $(EL2)^*$ , remained constant (see Sec. II).

(ii) The Fermi integral was calculated to get the free-electron concentration  $n$  in Eq. (4) with an assumption of a spherical and parabolic conduction band with pressure-dependent effective mass.<sup>34</sup>

The solid lines in Fig. 12, describing well the experimental data for both samples, represent the result of the best fit obtained for

$$\begin{aligned} \epsilon^{-/0}(p=0) - T \Delta S &= 14 \text{ meV}; \\ \frac{\partial \epsilon^{-/0}}{\partial p} &= -68 \text{ meV/GPa}. \end{aligned} \quad (5)$$

Since the temperature ( $T=35.1$  K) is low and  $\Delta S$  cannot be very high, this means that without pressure the  $[(EL2)^*]^{-/0}$  level is resonant with the conduction band and at  $p \approx 0.2$ – $0.3$  GPa it enters the energy gap; see Fig. 13, where we took  $\Delta S=0$ . Moreover, as is clear from



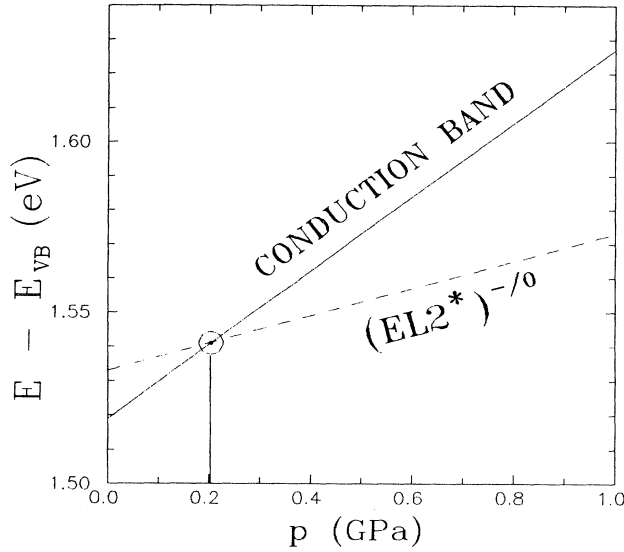


FIG. 13. The experimentally determined pressure dependence of the energetic position of the  $[(EL2)^*]^{-/0}$  level (see text) and the conduction-band (Ref. 35) with respect to the top of the valence band. The local entropy change of the transition  $[(EL2)^*]^{-/0} \rightarrow [(EL2)^*]^-$  was taken to be zero ( $\Delta S = 0$ ). The vertical line indicates the pressure at which the level enters the energy gap of GaAs.

Eqs. (2)–(4), we assumed that metastable  $EL2$  can trap under pressure only one extra electron (“positive- $U$ ” case). The excellent agreement between the experiment and the calculations clearly confirms the above assumption and excludes the possibility of the “negative- $U$ ” case [i.e., the trapping of two electrons by each  $(EL2)^*$  for which the total amount of electrons trapped on  $(EL2)^*$  for sample no. 2 would be two times higher than  $N_{EL2}$ ].

As is clear from our experimental results, the  $[(EL2)^*]^{-/0}$  level disappears when  $EL2$  recovers optically or thermally to its normal configuration. This fact needs some clarification. We know that  $EL2$  in our  $n$ -type samples can be in three different states, namely  $(EL2)^0$ ,  $[(EL2)^*]^0$ , and  $[(EL2)^*]^-$ . The total (electronic plus elastic) energies of these states are  $E_0$ ,  $E_0^*$ , and  $E_-^*$ , respectively. The first two correspond to neutral charge states with an electron at the bottom of the conduction band. The difference between  $E_-^*$  and  $E_0^*$ , defined as  $\varepsilon^{-/0}$  by Eq. (1), was determined in this section; see Eq. (5). The total energy of the neutral metastable  $EL2$  ( $E_0^*$ ) is certainly higher than its energy in the normal configuration ( $E_0$ ) with the difference  $\Delta E$ , which has not been experimentally determined (however, the theoretical prediction of Dąbrowski and Scheffler<sup>36</sup> gives  $\Delta E \approx 0.15$  eV and that of Chadi and Chang<sup>37</sup> gives 0.24 eV):

$$\Delta E = E_0^* - E_0 > 0. \quad (6)$$

The relative positions of  $E_0$ ,  $E_0^*$ , and  $E_-^*$  are schematically presented in Fig. 14. In both cases,  $p = 0$  and  $p > 0.3$  GPa, the stable state of  $EL2$  is the neutral charge state in the normal configuration. However, if  $EL2$  is

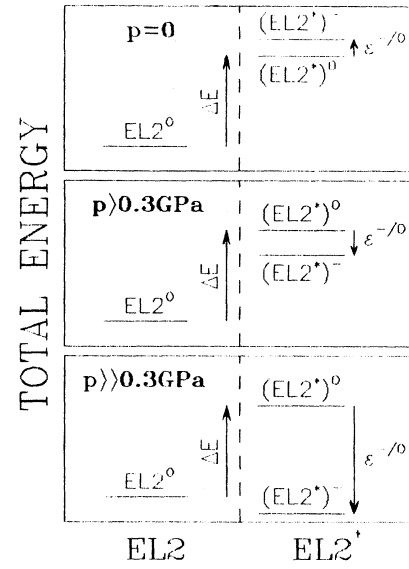


FIG. 14. The schematic diagram of the total energies of the three  $EL2$  defect states of both normal ( $EL2$ ) and metastable  $[(EL2)^*]$  configurations for various pressures.  $\varepsilon^{-/0}$  and  $\Delta E$  are defined in the text.

frozen in its metastable configuration  $(EL2)^*$  ( $T < 40$  K), it traps at  $p > 0.3$  GPa an additional electron because  $E_-^* < E_0^*$  in this case (i.e., the  $[(EL2)^*]^{-/0}$  level enters the energy gap). If the temperature is raised above  $T = 40$ – $50$  K the configuration barrier between  $EL2$  and  $(EL2)^*$  can be overcome and  $EL2$  returns to its normal configuration. At this sufficiently high temperature the capture of a free electron from the bottom of the conduction band, accompanied by the  $EL2 \rightarrow (EL2)^*$  transfer, would require relatively high energy:

$$\varepsilon^{-/0} + \Delta E = E_-^* - E_0. \quad (7)$$

This expression has the sense of the energy of some level that should be defined as the  $[(EL2)^*]^{-/0}/(EL2)^0$  level. At  $p = 0$ , this level is resonant and lies high in the conduction band. Thus, at high temperature, after the thermal equilibrium of  $EL2$  is restored, the  $[(EL2)^*]^{-/0}$  level disappears and is replaced by the completely empty  $[(EL2)^*]^{-/0}/(EL2)^0$  one. Nevertheless, because  $\partial \varepsilon^{-/0} / \partial p < 0$  (the pressure dependence of  $\Delta E$  is unfortunately unknown), at very high pressure ( $p \gg 0.3$  GPa; see Fig. 14) the left-hand side of Eq. (7) might become negative and in this case the stable state of  $EL2$  would be  $[(EL2)^*]^-$  and  $(EL2)^0$  would become the metastable one. If this was really observable, it would give a direct experimental method to estimate the value of  $\Delta E$ .

#### IV. CONCLUSIONS

Based on the above-described results of our high-pressure investigations of electrical conductivity and low-temperature DLTS, we have clearly shown that the metastable configuration of the  $EL2$  defect in  $n$ -type GaAs reveals electrical activity. We have proved that the only reliable explanation of this effect is the existence of

the  $[(EL2)^*]^{-/0}$  level, which is proper to the metastable  $EL2$  configuration. This level at  $p=0$  is resonant with the conduction band, and under relatively low (0.2–0.3 GPa) hydrostatic pressure it enters the energy gap capturing free electrons. The occupation of the level leads to the negatively charged state of the metastable configuration,  $[(EL2)^*]^-$ , which seems to be responsible for the recently discovered optical accessibility of the  $(EL2)^*$ .<sup>29</sup> The last effect manifests itself both in an extremely efficient purely optical full  $EL2$  recovery process (which can be monitored by electrical conductivity, low-temperature DLTS, or optical-absorption measurements) and in a weakly dispersive absorption linearly correlated with the concentration of the metastable  $EL2$ ,<sup>29</sup> which can now be easily interpreted as a photoionization of the  $[(EL2)^*]^{-/0}$  level. These findings strongly support our previous hypothesis<sup>29</sup> that both optical accessibility and electrical activity of the metastable  $EL2$  must exist jointly and that they are due to the population of the acceptorlike  $[(EL2)^*]^{-/0}$  level.

It should be pointed out that high-pressure measurements are a powerful experimental tool for studying the  $EL2$  metastable configuration, which was not directly accessible up to now. Since the  $[(EL2)^*]^{-/0}$  level population is always in thermal equilibrium with the conduction band, we deduced that the change of the charge state within the metastable configuration takes place without an additional strong lattice relaxation. Thus, from the investigations of the  $[(EL2)^*]^-$  state properties (which in particular should be paramagnetic and therefore EPR active), one can get direct information concerning the microscopic structure of the metastable  $EL2$  configuration as a whole, which is of crucial importance if one considers the model of the  $EL2$  defect and the mechanism of its metastability. Furthermore, our results have enabled us to determine quite precisely the energy of the  $[(EL2)^*]^{-/0}$  level and its pressure shift, as well as to exclude the “negative- $U$ ” situation for this level. We have explained the observed effects of the appearance and disappearance of the  $[(EL2)^*]^{-/0}$  level exactly correlated with the distribution of the  $EL2$  between its metastable and normal configurations and suggested the existence of the  $[(EL2)^*]^-/(EL2)^0$  level, which lies higher than the  $[(EL2)^*]^{-/0}$  one, with the separation between both levels being  $\Delta E$ , which is the total energy difference between neutral  $EL2$  in the normal and metastable configurations. We have also pointed out that pressure experiments might help to determine the value of  $\Delta E$ .

Moreover, it is worth mentioning that we have found out some other qualitatively new physical phenomenon closely related to the existence of this level. We have shown that one can observe a light-induced metal-insulator transition—the process of optical  $EL2$  quenching involves at high pressure a drastic fall of the concentration of conducting electrons bound on photon-created metastable  $EL2$ , and therefore leads to the conversion of a sample from a highly conductive to a semi-insulating

one. Additionally, a successive application of the  $EL2$  photoquenching and photorecovery processes gives us a very unique possibility of controlling the number of deep defect centers (metastable  $EL2$ ) that can bind free electrons on the localized electronic state.

We would like to emphasize that the existence of the  $[(EL2)^*]^{-/0}$  level is now well established and this experimental fact must be taken into account by any theoretical model of  $EL2$ . Unfortunately, our experimental results do not provide any direct insight into the microscopic structure of the  $EL2$  defect and particularly they cannot distinguish between the two most popular  $EL2$  models, namely that of the isolated  $As_{Ga}$  (Refs. 36–39) and that of the  $As_{Ga}-As_i$  pair.<sup>14,39–42</sup> Since, in our opinion, the isolated  $As_{Ga}$  model better explains most of the experimentally established  $EL2$  properties, we have adopted the commonly accepted assumption and used it throughout this paper that the main  $EL2$  midgap donor level is the  $(0/+)$  one [this is in contradiction with the  $As_{Ga}-As_i$  model, which claims that this should be a  $(+/++)$  level]. It should be pointed out that Dąbrowski and Scheffler<sup>36,39</sup> say that the isolated  $As_{Ga}$  model predicts that the metastable  $EL2$  configuration ( $As_i-V_{Ga}$ ), being in its neutral charge state, possesses an interstitial-like empty state of  $a$  symmetry (labeled as  $1a$  in Ref. 36), which can be filled with an additional electron. The corresponding  $(-/0)$  level was found to be close to the bottom of the conduction band. This is a very good candidate for our  $[(EL2)^*]^{-/0}$  level. Since the population of the level means simply filling the  $1a$  state with one electron, the degeneracy factor of this level must be equal to 2. This implies that in Eq. (5), from Sec. III B,  $\Delta S = k \ln 2$  and  $\epsilon^{-/0}(p=0) \approx 16$  meV (the temperature at which the experiment was performed was  $T = 35.1$  K). Nevertheless, the  $As_{Ga}-As_i$  model cannot be ruled out because it also admits the existence of a level lying close to the conduction-band edge but in this case this would be the  $(0/+)$  one. This level originates from the filling of the  $e$  symmetry state whose wave function is largely localized on the interstitial arsenic.<sup>14,39,42</sup>

The major discrepancy between the above-mentioned models concerns the predictions of the microscopic structure of the metastable  $EL2$  configuration. Therefore the direct investigations of metastable  $EL2$ , which are now feasible due to its optical, electrical, and expected EPR activity, induced by pressure, should finally solve the problem of the  $EL2$  atomic identification.

#### ACKNOWLEDGMENTS

We are indebted to Professor J. Lagowski for one of the investigated samples. This work was supported by the Central Program for Fundamental Research Contract No. CPBP-01.05 of the Polish Ministry of National Education.

- <sup>1</sup>J. Lagowski, D. G. Lin, T. Aoyama, and H. C. Gatos, Appl. Phys. Lett. **44**, 336 (1984).
- <sup>2</sup>M. Skowronski, J. Lagowski, and H. C. Gatos, J. Appl. Phys. **59**, 2451 (1986).
- <sup>3</sup>R. Bray, K. Wan, and J. C. Parker, Phys. Rev. Lett. **57**, 2434 (1986).
- <sup>4</sup>M. Hoinkis, E. R. Weber, W. Walukiewicz, J. Lagowski, M. Matsui, H. C. Gatos, B. K. Meyer, and J. M. Spaeth, Phys. Rev. B **39**, 5538 (1989).
- <sup>5</sup>G. M. Martin, Appl. Phys. Lett. **39**, 747 (1981).
- <sup>6</sup>A. Chantre, G. Vincent, and P. Bois, Phys. Rev. B **23**, 5335 (1981).
- <sup>7</sup>M. Kaminska, M. Skowronski, J. Lagowski, J. M. Parsey, and H. C. Gatos, Appl. Phys. Lett. **43**, 302 (1983).
- <sup>8</sup>B. Dischler, F. Fuchs, and U. Kaufmann, Appl. Phys. Lett. **48**, 1282 (1986).
- <sup>9</sup>F. Fuchs and B. Dischler, Appl. Phys. Lett. **51**, 2115 (1987).
- <sup>10</sup>M. Skowronski, J. Lagowski, and H. C. Gatos, Phys. Rev. B **32**, 4264 (1985).
- <sup>11</sup>J. C. Parker and R. Bray, Phys. Rev. B **38**, 3610 (1988).
- <sup>12</sup>E. R. Weber, H. Ennen, U. Kaufmann, J. Windscheif, J. Schneider, and T. Wosinski, J. Appl. Phys. **53**, 6140 (1982).
- <sup>13</sup>M. Baeumler, U. Kaufmann, and J. Windscheif, Appl. Phys. Lett. **46**, 781 (1985).
- <sup>14</sup>H. J. von Bardeleben, D. Stievenard, D. Deresmes, A. Huber, and J. C. Bourgoin, Phys. Rev. B **34**, 7192 (1986).
- <sup>15</sup>G. M. Martin and S. Makram-Ebeid, in *Deep Centers in Semiconductors*, edited by S. T. Pantelides (Gordon and Breach, New York, 1986), p. 399.
- <sup>16</sup>A. Mittoneau and A. Mircea, Solid State Commun. **30**, 157 (1979).
- <sup>17</sup>G. Vincent, D. Bois, and A. Chantre, J. Appl. Phys. **53**, 3643 (1982).
- <sup>18</sup>P. Trautman, M. Kaminska, and J. M. Baranowski, Cryst. Res. Technol. **23**, 413 (1988); Acta Phys. Polon. **A71**, 269 (1987).
- <sup>19</sup>D. W. Fischer, Phys. Rev. B **37**, 2968 (1988).
- <sup>20</sup>T. Sugiyama, K. Tanimura, and N. Itoh, Appl. Phys. Lett. **55**, 639 (1985).
- <sup>21</sup>D. W. Fischer, Appl. Phys. Lett. **50**, 1751 (1987).
- <sup>22</sup>J. C. Parker and R. Bray, Phys. Rev. B **37**, 6368 (1988).
- <sup>23</sup>M. Tajima, K. Saito, T. Ino, and K. Ishida, Jpn. J. Appl. Phys. Pt. 2 **27**, L101 (1988).
- <sup>24</sup>M. O. Manasreh and D. W. Fischer, Phys. Rev. B **39**, 13001 (1989).
- <sup>25</sup>Y. Mochizuki and T. Ikoma, Jpn. J. Appl. Phys. Pt. 2 **24**, L895 (1985).
- <sup>26</sup>X. Boddaert, D. Stievenard, and J. C. Bourgoin, Phys. Rev. B **40**, 1051 (1989).
- <sup>27</sup>M. Tajima, Jpn. J. Appl. Phys. Pt. 2 **23**, L690 (1984).
- <sup>28</sup>M. Tajima, Jpn. J. Appl. Phys. Pt. 2 **24**, L47 (1985).
- <sup>29</sup>M. Baj and P. Dreszer, Phys. Rev. B **39**, 10470 (1989).
- <sup>30</sup>J. Lagowski, H. C. Gatos, C. H. Kang, M. Skowronski, K. Y. Ko, and D. G. Lin, Appl. Phys. Lett. **49**, 892 (1986).
- <sup>31</sup>G. Vincent, A. Chantre, and D. Bois, J. Appl. Phys. **50**, 5484 (1979).
- <sup>32</sup>D. Pons and S. Makram-Ebeid, J. Phys. (Paris) **40**, 1161 (1979).
- <sup>33</sup>S. Makram-Ebeid and M. Lanoo, Phys. Rev. B **25**, 6406 (1982).
- <sup>34</sup>J. S. Blakemore, J. Appl. Phys. **53**, 10 (1982).
- <sup>35</sup>D. J. Wolford, in *Proceedings of the 18th International Conference on the Physics of Semiconducting Compounds, Stockholm, 1986*, edited by O. Engström (World Scientific, Göteborg, 1987), Vol. 2, p. 1115.
- <sup>36</sup>J. Dąbrowski and M. Scheffler, Phys. Rev. B **40**, 10391 (1989).
- <sup>37</sup>D. J. Chadi and K. J. Chang, Phys. Rev. Lett. **60**, 2187 (1988).
- <sup>38</sup>J. Dąbrowski and M. Scheffler, Phys. Rev. Lett. **60**, 2183 (1988).
- <sup>39</sup>J. Dąbrowski and M. Scheffler, Mater. Sci. Forum **38-41**, 51 (1989).
- <sup>40</sup>B. K. Meyer, D. M. Hofmann, J. R. Niklas, and J. M. Spaeth, Phys. Rev. B **36**, 1332 (1987).
- <sup>41</sup>G. A. Baraff and M. Schlüter, Phys. Rev. B **35**, 6154 (1987).
- <sup>42</sup>G. A. Baraff, M. Schlüter, and M. Lanoo, Mater. Sci. Forum **38-41**, 91 (1989).